International Journal of Engineering and Technology Vol. 1, No. 2, June, 2009
1793-8236

# Thermal Sensitivity Coefficients of The Fabrication Materials Based A thermal Arrayed Waveguide Grating (AWG) in Wide Area Dense Wavelength Division Multiplexing Optical Networks

Abd El–Naser A. Mohammed, Ahmed Nabih Zaki Rashed, Abd El–Fattah A. Saad

***Abstract*—In the present paper, the study of the thermal sensitivity coefficients of the three different fabrication materials based a thermal Arrayed Waveguide Grating (AWG) under the spectral wavelength and ambient temperature sensing in wide area dense wavelength division multiplexing optical access network based on the MATLAB (Mathematical laboratory) curve fitting program.**

***Index Terms*—Conventional Arrayed waveguide Grating (AWG), Silica-doped material, Polymethyl-metha acrylate (PMMA) Polymer material, Lithium Niobate (LiNbO3) material, Thermal Sensitivity Coefficients.**

## I. INTRODUCTION

With the increasing diversity of Dense Wavelength Division Multiplexing (DWDM) systems in recent years, the needs facing the Arrayed Waveguide Grating (AWG), which handles the function of wavelength multiplexer/demultiplexer, is for a thermalization (temperature-independence) requiring no power supply. This would make it possible for the AWG module to be isolated from transmission devices inside an office and to be installed in a variety of locations having no power supply, making them able to satisfy the needs of the increasingly diversified optical communications networks of the future [1]. The arrayed-waveguide grating (AWG) is an extremely versatile device that features and combines simultaneously unique periodic spatial and frequency properties and the possibility of integration on a chip. Examples of the production of spectrum-sliced sources, dispersion compensation, wavelength division multiplexing (WDM) multiplexers and demultiplexers, tunable filters, wavelength routing, as in the image process and optical processing [2, 3]. The Silica-doped germanium based arrayed-waveguide grating (AWG) multi/demultiplexer is a key optical access networking for constructing Dense Wavelength Division-Multiplexing (DWDM) systems. An a thermal AWG must be developed if we are to expand the AWG application area to access networks [4]. This is because the center wavelength of a conventional silica-based AWG shifts with temperature fluctuation, and so a temperature stabilizing part such as a thermoelectric cooler must be incorporated in the AWG package. One approach uses polymers whose temperature coefficients have negative values with another approach, the input waveguide position moves as a result of the thermal expansion of compensation metal. The explosive growth of Internet traffic is pushing the rapid development of high-speed broadband optical networks, such as dense wavelength-division multiplexing (DWDM) systems. In these optical networks, a variety of optical components such as wavelength-division multi/demultiplexers (MUX/DEMUXs), erbium-doped fiber amplifiers (EDFAs), lasers, photodetectors, and modulators are indispensable for constructing optical networks. Among others, arrayed waveguide grating (AWG)-type MUX/DEMUXs based on planar lightwave circuits (PLCs) have played an important role as a key optical component for DWDM. Meanwhile, in the midst of the telecom winter, many carriers are struggling to reduce per-bit cost. Therefore, optical components are expected to have new functions that reduce the operational and capital expenditures. For example, an AWG itself is expected to be a thermal as well as low cost. In order to lower the cost of AWGs, besides testing and packaging costs [5], chip size is quite important because the number of AWGs laid out over a wafer determines the general cost. This is especially true for large-size optical circuits such as AWGs. The increase in refractive index difference between the core and cladding is a quite useful way to reduce chip size. From the practical point of view, however, when a high-contrast waveguide is used, the coupling loss between the waveguide and fiber that results from mode-field mismatch increases, and this should be reduced. Avoiding the addition of further processes is desirable when applying these schemes in order to maintain low cost. It needs no special process treatment and achieves low coupling loss. In addition to that, combined high-contrast AWG waveguides with the a thermal structure by introducing crescent trenches with an adhesive into the slab waveguide of an AWG. The arrayed waveguide grating (AWG) multiplexer is a key device for dense wavelength division multiplexing (DWDM) in optical telecommunication systems. An NxN

Rashed is with Electronics and Electrical Communication Engineering Department, faculty of Electronic Engineering, Menouf 32951, Menoufia University, EGYPT. Corresponding author to provide phone. [Tel.: +2 048-3660-617, Fax: +2 048-3660-617].

AWG multiplexer can offer some basic functions including multiplexing, demultiplexing, routing and NxN interconnection. Polymer AWG devices possess some excellent particular features including easier fabrication and easier control of the refractive index compared with AWGs made of other materials. Recently, many research groups have focused on the development of polymer AWG multiplexers, and have fabricated such optical devices using various polymeric materials. Excellent AWG devices are dependent on accurate structural design and fine technological processing. However, fabrication errors are hard to avoid in the manufacturing of the AWG devices. Some previous researches also reported on the impact of fabrication errors on the transmission characteristics of AWG devices. Therefore, parameter optimization and fabrication error analysis are very important in the design and fabrication of AWG devices. Passive optical networks (PON) are a key technology to enable the development of an optical access network. Currently there are many versions of PON technology. This in the 1980s, the technology was furthered with the development of the Broadband PON to carry broadband data over 20 km to 32 customers at symmetrical data rates of up to 622 Mbit/s. The IEEE has also developed a PON architecture as part of the Ethernet in the First Mile project. Ethernet-PON (EPON) are capable of delivering Ethernet encapsulated data at a rate of 1 Gbit/s symmetrical with commercially available systems demonstrating 64 users over a range of up to 20 km. However, the highest capacity standardized PON architecture is the Gigabit-PON standardized by the ITU-T, which is capable of operating at 2.5 Gbit/s symmetrical data rates, connecting up to 64 customers over 20 km [6], although currently only lower rates (1.25 Gbit/s) in the upstream are commercially available. Traditionally PONs are connected to the core telecoms network through SDH rings which form the metro network. The need for high speed transmission and the exchange of large amount of information has been motivated to increase the capacity of the optical fiber communication system. WDM (wavelength division multiplexing) optical communication system has been the active areas of research worldwide, utilizing a single fiber to transmit multi-wavelength channel data, in order to accommodate the increasing need for larger information transmission. Precise wavelength selection technology is one of the key technologies for the successful realization of the WDM optical system. Since the optical channel add/drop function is required in the WDM system in addition to the simple point-to-point data transmission, optical wavelength selection technology is the key technology in the WDM system. Also, for the realization of Tb/s rate optical ATM switching network, development of wavelength selection technology is essential which will be the basic component for wavelength multiplexing and demultiplexing. One of the components to realize such function is a wavelength division multiplexing with an arrayed waveguide grating (AWG) using silica [7], polymer, or InP materials. Silica-based devices have large dimensions compared to the InP-based devices, due to the low index contrast and the corresponding large bending radii, and it makes them less suitable for integration of large numbers of components. Also, due to passive character of silica, it has a limited potential for integration of active components. However, the main advantage of InP-based devices lies in their potential for monolithic integration of active components, even though they exhibit higher propagation. In wavelength division multiplexing (WDM) systems with large number of channels, there is the need of inserting a large number of channels in a single optical fiber. For this purpose, several devices have been developed, and the arrayed-waveguide grating (AWG) has been indicated as a proper choice. This is due to the properties of such a device and to the simplicity of manufactory. However, there are limitations in the use of *AWG* devices in dense WDM (DWDM) systems. One of these limitations is related to the value of free spectral range (FSR), which reduces the number of channels multiplexed or demultiplexed. Other limitation is related with the small isolation between channels that this kind of device can provide. Taking this into account, it is desirable to have a method of determining the AWG physical dimensions that lead to the channel spacing and full width half maximum (FWHM) required for all the channels of the DWDM system [8].

In the present study, we have investigated the thermal sensitivity coefficients of the fabrication materials based conventional arrayed waveguide grating (AWG) in wide area dense wavelength division multiplexing optical access networks.

## II. AWG IN DENSE WAVELENGTH-DIVISION MULTIPLEXING OPTICAL NETWORKS

Arrayed waveguide grating (AWG) which handles the function of wavelength multiplexer/demultiplexer is extensively used in configuring optical communication networks that are becoming more diversified. Since the transmission wavelength of an AWG is temperature dependent, it was a common practice to control its temperature using heaters or Peltier elements. But this caused problems of power consumption increase in the whole system in addition to limiting the installation locations of AWGs, thus making it difficult to respond to various needs of the next-generation optical communication networks, despite the fact that system performance upgrading and function enhancement are required in recent years. In the optical fiber communication area, it is expected that broadband network provision will require thousands of optical fibers to be accommodated in a central office (CO) for the optical access network. Optical fiber is capable of delivering bandwidth-intensive integrated, voice, data and video services at distance beyond 20 km in the subscriber access network. All transmission in a Optical Access Network is performed between an optical line terminal (OLT) and optical network unit (ONU). The OLT resides in the central office, connecting the optical access network to the metro back-bone, and the ONU is located the end-user location. Optical fiber maintenance is a very important issue to be consider in a developing a high quality and reliable Optical Access Network. The long feeder line in a Optical Access Network is a vulnerable part of the network; when unprotected, a break of it puts the whole Optical access network out of service. One types of network protection have been described in ITU-T

Recommendation G.983.1, Protection of the feeder fiber only by a spare fiber over which the traffic can be rerouted by means of optical switches. After detection of a failure in the primary fiber and switch-over to the spare fiber, also reranging has to be done by the Optical access network transmission convergence (TC) layer. To support various optical communication network services expected in the coming years, there has been much effort to develop a fiber to the home (FTTH) access optical network. FTTH-Optical access network offers many advantages such as high speed, large capacity, and low cost. However, despite its advantages, a typical FTTH-Optical access network with the feeder fiber architecture does not have self-monitoring capability. Preventive monitoring on the optical level can save a considerable amount of operational cost. Monitoring tool for detecting failure in optical fiber networks is traditionally set up on dark fiber as this provides good balance between material cost, system provisioning effort and fault detection success rate. Most monitoring systems used for physical fault detection and positioning employ optical time domain reflect meter (OTDR).

## III. MODELING BASIS AND ANALYSIS

### A. SILICA-DOPED MATERIAL (SIO2(1-X)+GEO2(X))

The Sellmeier equation of the refractive-index is the form [9]:

$$n^2 = 1 + \frac{B_1 l^2}{l^2 - B_2^2} + \frac{B_3 l^2}{l^2 - B_4^2} + \frac{B_5 l^2}{l^2 - B_6^2} \qquad (1)$$

where λ is the optical wavelength (μm), and the coefficients of Eq. (1) is given by [9].

$B_1$= 0.691663+0.1107001* x,

$B_2$= (0.0684043+0.000568306 * x)$^2$ * (T/$T_0$)$^2$

$B_3$= 0.4079426+0.31021588 * x,

$B_4$= (0.1162414+0.03772465 * x)$^2$ * (T/$T_0$)$^2$

$B_5$= 0.8974749-0.043311091 * x,

$B_6$= (9.896161+1.94577 * x)$^2$

where x is the Germania mole fraction, T is the temperature of the material, K, and $T_0$ is the reference temperature (300 K). The differentiation of Eq. (1) w. r. t. Temperature (T) yields:

$$\frac{\partial n}{\partial T} = \left(-l^2/n\right)\left[\frac{B_1 B_2 \frac{\partial B_2}{\partial T}}{\left(l^2 - B_2^2\right)^2} + \frac{B_3 B_4 \frac{\partial B_4}{\partial T}}{\left(l^2 - B_4^2\right)^2} + \frac{B_5 B_6 \frac{\partial B_6}{\partial T}}{\left(l^2 - B_6^2\right)^2}\right] \qquad (2)$$

### B. POLYMETHYL-METHA ACRYLATE (PMMA) POLYMER MATERIAL

The Sellmeier equation of the refractive-index is the form of [10]:

$$n^2 = 1 + \frac{C_1 l^2}{l^2 - C_2^2} + \frac{C_3 l^2}{l^2 - C_4^2} + \frac{C_5 l^2}{l^2 - C_6^2} \qquad (3)$$

where λ is in μm, and the coefficients of Eq. (3) is given [10]. $C_1$= 0.4963, $C_2$= 71.80 x $10^{-3}$, $C_3$= 0.6965, $C_4$= 117.4 x $10^{-3}$, $C_5$= 0.3223, $C_6$= 9237 x$10^{-3}$.

Also, the differentiation of Eq. (3) w. r. t. Temperature (T) gives:

$$\frac{\partial n}{\partial T} = \left(-l^2/n\right)\left[\frac{C_1 C_2 \frac{\partial C_2}{\partial T}}{\left(l^2 - C_2^2\right)^2} + \frac{C_3 C_4 \frac{\partial C_4}{\partial T}}{\left(l^2 - C_4^2\right)^2} + \frac{C_5 C_6 \frac{\partial C_6}{\partial T}}{\left(l^2 - C_6^2\right)^2}\right] \qquad (4)$$

### C. LITHIUM NIOBATE (LINBO3) MATERIAL

The set of parameters required to completely characterize the wavelength dependence of the refractive-index (n)is given, where Sellmeier equation of the refractive-index is the form [11]:

$$n^2 = A_1 + A_2 H + \frac{A_3 + A_4 H}{l^2 - \left(A_5 + A_6 H\right)^2} + \frac{A_7 + A_8 H}{l^2 - A_9^2} - A_{10} l^2 \qquad (5)$$

where λ is in μm and $H = T^2 - T_0^2$ . T is the temperature of the material, K, and $T_0$ is the reference temperature and is considered 300 K. The set of parameters is recast and dimensionally adjusted as below [11].

$A_1$=5.35583, $A_2$=4.629 x $10^{-7}$, $A_3$=0.100473, $A_4$=3.862 x $10^{-8}$, $A_5$=0.20692, $A_6$=-0.89 x $10^{-8}$, $A_7$=100, $A_8$=2.657 x $10^{-5}$, $A_9$=11.34927, $A_{10}$=0.015334. Equation (5) can be simplified as:

$$n^2 = A_{12} + \frac{A_{34}}{l^2 - A_{56}^2} + \frac{A_{78}}{l^2 - A_9^2} - A_{10} l^2 \qquad (6)$$

where: $A_{12}=A_1+A_2H$, $A_{34}=A_3+A_4H$, $A_{56}=A_5+A_6H$, $A_{78}=A_7+A_8H$. Then the differentiation of Eq. (6) w. r. t. Temperature (T) gives:

$$\frac{\partial n}{\partial T} = \left(\frac{T}{n}\right)\left[A_2 + \frac{\left(l^2 - A_{56}^2\right)A_4 + 2A_6 A_{56} A_{34}}{\left(l^2 - A_{56}^2\right)^2} + \frac{A_8}{\left(l^2 - A_9^2\right)}\right] \qquad (7)$$

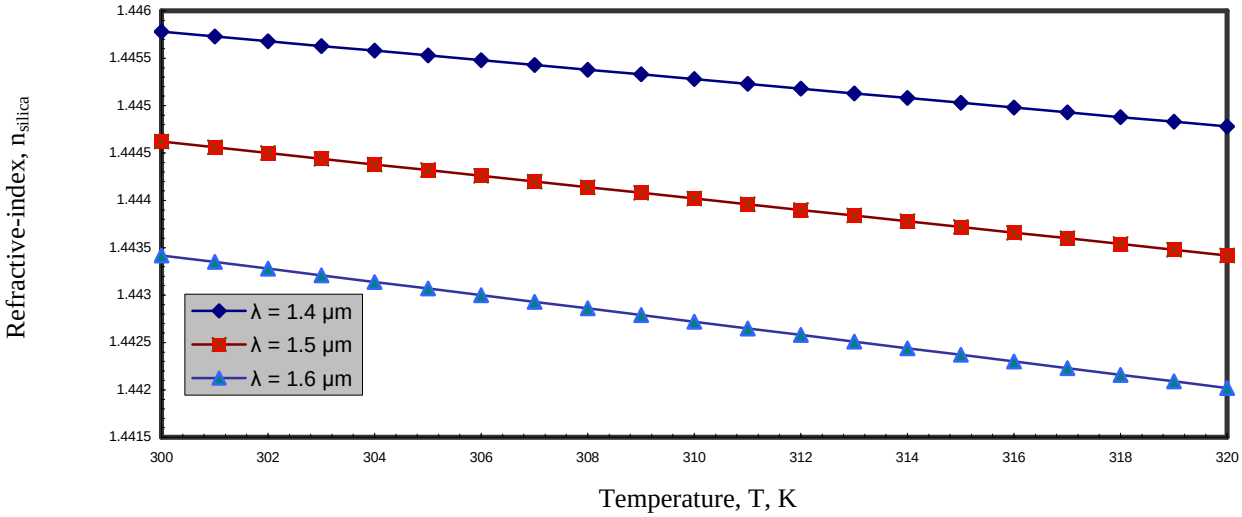


Fig. 1. Variation of refractive-index (n) Versus temperature for Silica-doped Material.

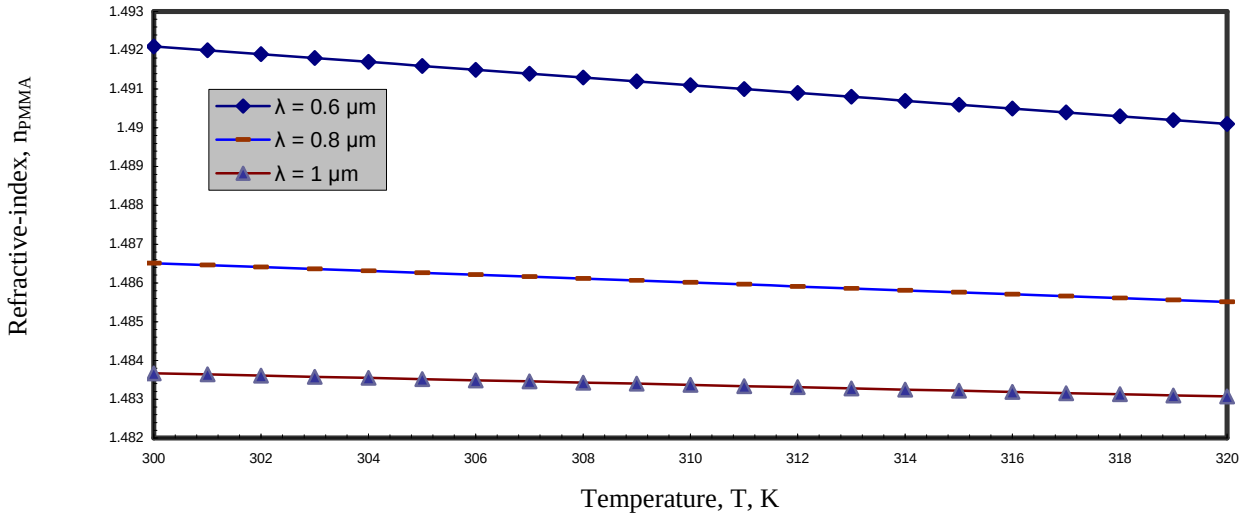


Fig. 2. Variation of refractive-index (n) Versus temperature for PMMA Polymer Material.

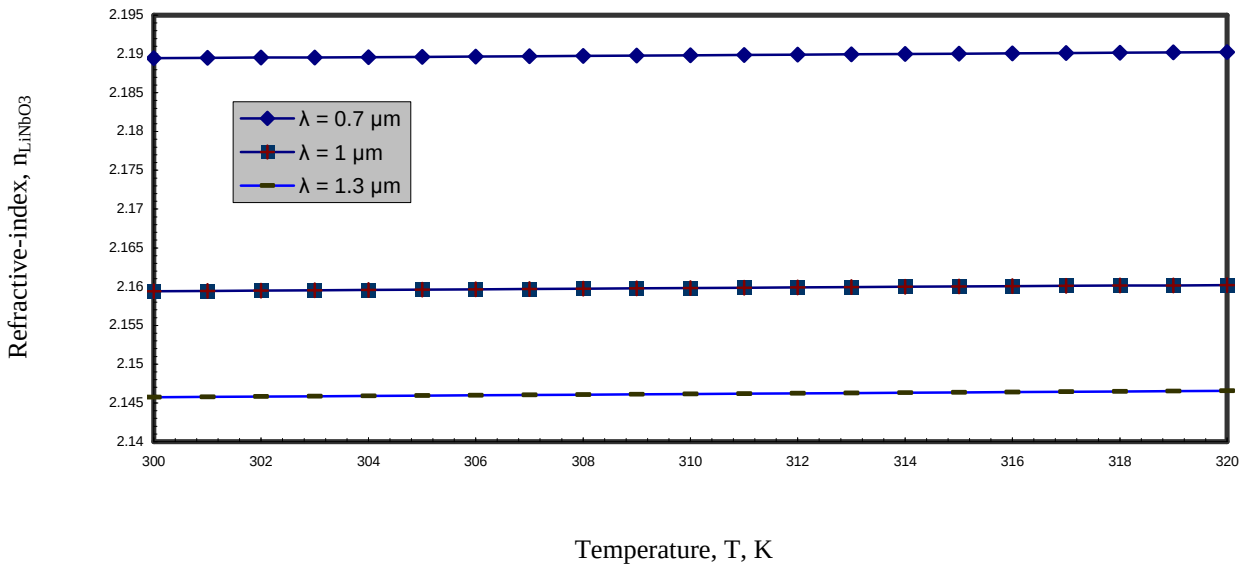


Fig. 3. Variation of refractive-index (n) Versus temperature for LiNbO3 Material.

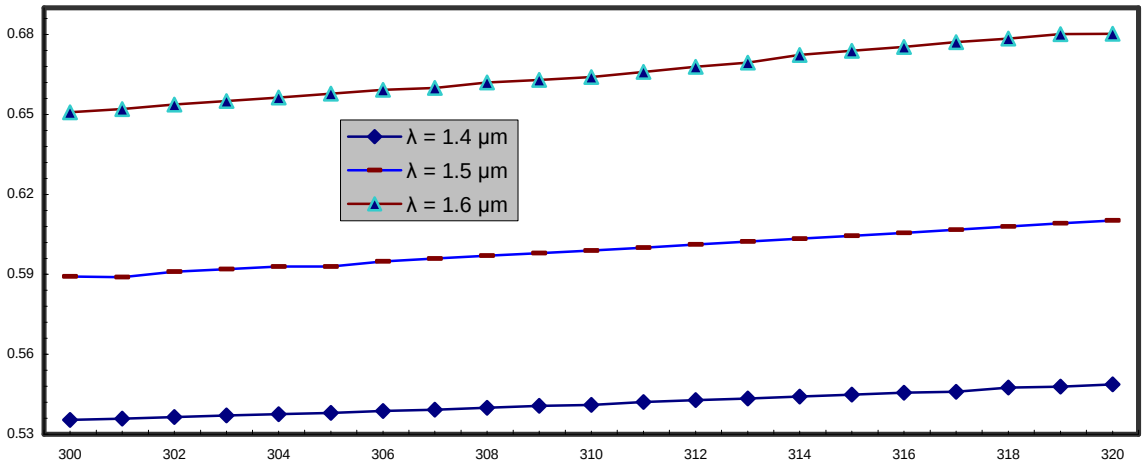


Fig. 4. Variation of dn/dT Versus temperature for Silica-doped Material

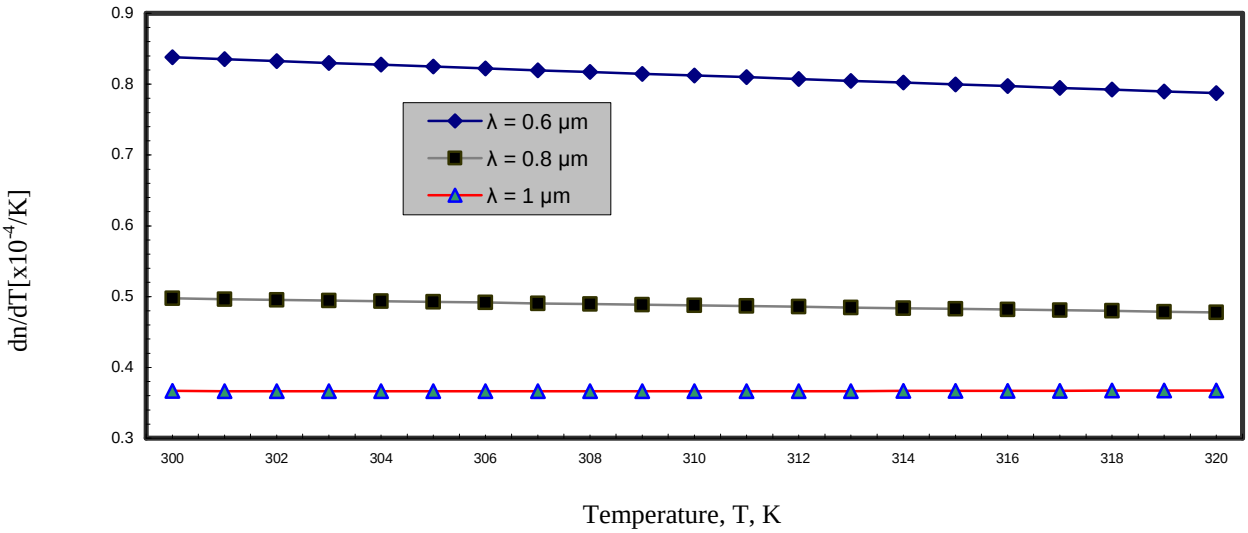


Fig. 5. Variation of dn/dT Versus temperature for PMMA Polymer Material

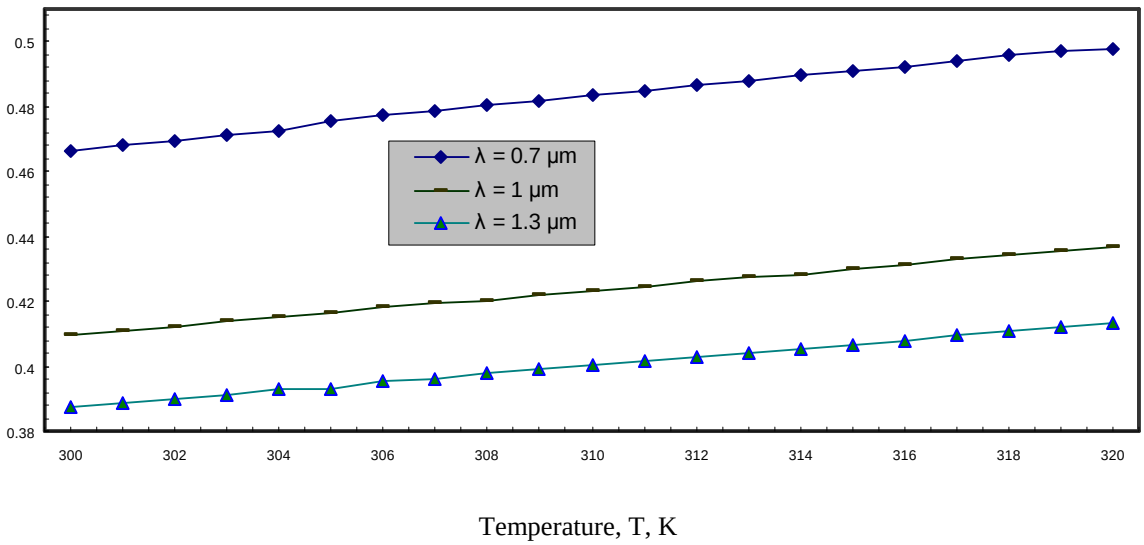


Fig. 6. Variation of dn/dT Versus temperature for LiNbO3 Material

## IV. ANALYSIS OF THE RESULTS

1) As shown in Figs. (1- 3) indicate that:
As the temperature of the waveguide material (T) increases, refractive-index (n) of the material decreases in the the two fabrication materials for waveguide (Silica-doped, PMMA), but in the case of $LiNbO_3$ increases at the constant wavelength (λ).
2) As shown in Fig. 4, we can fit the relation between the variation of the refractive-index w. r. t the variation of Temperature (dn/dT) as a function of three terms based on MATLAB curve-fitting program [9]:

$$\frac{dn}{dT} = d_0 + d_1\, l + d_2\, l^2 \qquad (8)$$

The fitting based on no. of 17 points iteration [at the starting wavelength (1.3 μm), with step-size variation of (0.025 μm), and the ending wavelength (1.7 μm)] for the Silica-doped material [see Appendix A]. Then we can fit the sensitivity coefficients ( $d_0, d_1, d_2$ ) as a function of the Temperature (T).

$$d_0 = 0.72x10^{-2} - 0.46x10^{-4}T + 0.74x10^{-7}T^2 \qquad (9)$$

$$d_1 = -0.7x10^{-2} - 0.45x10^{-4}T + 0.72x10^{-7}T^2 \qquad (10)$$

$$d_2 = 0.1x10^{-2} - 0.63x10^{-5}T + 0.99x10^{-8}T^2 \qquad (11)$$

Then the variation of the refractive-index w. r. t variation of Temperature (dn/dT) in the form:

$$\frac{dn}{dT} = \begin{bmatrix} d_0 & d_1 & d_2 \end{bmatrix} \begin{bmatrix} 1 \\ l \\ l^2 \end{bmatrix} \qquad (12)$$

In fact, the Thermal sensitivity is given: ( $S_T^n = a\,\frac{dn}{dT}$ ), $a = \frac{T}{n}$, and as shown in Figs. (1, 4), as the Temperature of the material (T) increases, then the refractive-index of material (n) decreases, (dn/dT) increases, and α also increases, this achieve high thermal sensitivity for Silica-doped material than two other materials (PMMA, $LiNbO_3$).

3) As shown in Fig. 5, we can fit the relation between the variation of the refractive-index w. r. t the variation of Temperature (dn/dT) as a function of three terms based on MATLAB curve-fitting program [9]:

$$\frac{dn}{dT} = h_0 + h_1 l + h_2\, l^2 \qquad (13)$$

The fitting based on no. of 17 points iteration [at the starting wavelength (0.4 μm), with step-size variation of (0.05 μm), and the ending wavelength (1.2 μm)] for the PMMA Polymer material [see Appendix B]. Then we also can fit the sensitivity coefficients ( $h_0, h_1, h_2$ ) as a function of the Temperature (T).

$$h_0 = 0.13x10^{-2} - -0.42x10^{-5}T + 0.41x10^{-8}T^2 \qquad (14)$$

$$h_1 = -0.3x10^{-2} + 0.12x10^{-4}T - 0.13x10^{-7}T^2 \qquad (15)$$

$$h_2 = 0.16x10^{-2} - 0.65x10^{-5}T + 0.82x10^{-8}T^2 \qquad (16)$$

Then the variation of the refractive-index w. r. t variation of the Temperature (dn/dT) in the form:

$$\frac{dn}{dT} = \begin{bmatrix} h_0 & h_1 & h_2 \end{bmatrix} \begin{bmatrix} 1 \\ l \\ l^2 \end{bmatrix} \qquad (17)$$

In fact, the Thermal sensitivity is given: ( $S_T^n = b\,\frac{dn}{dT}$ ), $b = \frac{T}{n}$, and as shown in Figs. (2, 5), as the Temperature of the material (T) increases, then the refractive-index of material (n) decreases, (dn/dT) decreases, and this achieve low thermal sensitivity for PMMA Polymer material.

(4) As shown in Fig. 6, we can fit the relation between the variation of the refractive-index w. r. t the variation of Temperature (dn/dT) as a function of three terms based on MATLAB curve-fitting program [9]:

$$\frac{dn}{dl} = y_0 + y_1 T + y_2 T^2 \qquad (18)$$

The fitting based on no. of 17 points iteration [at the starting wavelength (0.4 μm), with step-size variation of (0.075 μm), and the ending wavelength (1.6 μm)] for the $LiNbO_3$ material [see Appendix C]. Then we also can fit the sensitivity coefficients ( $y_0, y_1, y_2$ ) as a function of the Temperature (T).

$$y_0 = -0.12x10^{-2} - 0.77x10^{-5}T - 0.12x10^{-7}T^2 \qquad (19)$$

$$y_1 = 0.31x10^{-2} - 0.2x10^{4}T + 0.32x10^{-7}T^2 \qquad (20)$$

$$y_2 = -0.15x10^{-2} + 0.1x10^{-4}T - 0.16x10^{-7}T^2 \qquad (21)$$

Then the variation of the refractive-index w. r. t variation of the Temperature (dn/dT):

$$\frac{dn}{dT} = \begin{bmatrix} y_0 & y_1 & y_2 \end{bmatrix} \begin{bmatrix} 1 \\ l \\ l^2 \end{bmatrix} \qquad (22)$$

In fact, the Thermal sensitivity is given: ( $S_T^n = y\,\frac{dn}{dT}$ ), $y = \frac{T}{n}$, and as shown in Figs. (3, 6), as the Temperature of the material (T) increases, then the refractive-index of material (n) increases, (dn/dT) decreases, and this achieve moderate thermal sensitivity for $LiNbO_3$ material.

## V. CONCLUSIONS

Silica-doped material is the preferred fabrication materials for the based waveguides employed in conventional arrayed waveguide grating (AWG) for wide area dense wavelength-division multiplexing optical access networks. So that Silica-doped has the lowest refractive-index than the two other materials (PMMA, $LiNbO_3$), therefore the high the speed of the light through its based fabrication waveguide material. But Silica-doped has the high thermal sensitivity, and low thermal stability than the two fabrication materials, that is the only drawback in silica-doped fabrication material. PMMA, and $LiNbO_3$ have low, moderate thermal sensitivity, moderate, and low thermal stability respectively at the interval of the wavelengths (0.4 μm-1.2 μm), and (0.4 μm-1.6 μm), so that the PMMA and $LiNbO_3$ are the preferred fabrication materials based a thermal AWG.

## REFERENCES

[1] T. Saito et al.; Furukawa Review, "Development of A Heater-Control Arrayed Wane guide Grating (AWG) Module", Vol. 47, No. 22, pp. 1-5, 2002.
[2] T. Saito et al.; Furukawa Review, "Ultra-Low-Loss A thermal AWG Module With A Large Number of Channels", Vol. 20, No. 26, pp. 1-5, 2004.
[3] Y. Kokubun, and S. Taga, "Three-Dimensional A thermal Waveguides for Temperature Independent Lightwave Devices, " Electron. Lett., Vol. 30, pp. 1223–1225, 1994.
[4] Y. Inoue, A. Kaneko, F. Hanawa, H. Takahashi, K. Hattori, and S. Sumida, "A thermal silica-Based Arrayed-Waveguide Grating (AWG), " Electron. Lett., Vol. 33, pp. 1945–1946, 1997.
[5] K. Maru, M. Ohkawa, H. Nounen, S. Takasugi, S. Kashimura, H. Okano, and H. Uetsuka, "A thermal and Center Wavelength Adjustable Arrayed Waveguide Grating, " in Tech. Dig. OFC 2000, Paper WH3, Vol. 2, pp. 130–132, 2000.
[6] K. A. Ackerman, K. A. Paget, L. F. Schneemeyer, L. J.-P. Ketelsen, O. Sjolund, J. E. Graebner, A. Kanan, F. W. Warning, V. R. Raju, L. Eng, E. D. Schaeffer, and P. Van Emmerik, "Low-Cost A thermal Wavelength Locker Integrated in a Temperature-Tuned Laser Package, " in Tech. Dig.OFC 2003, Post deadline Paper PD32-1, Vol. 2 pp. 130–132, 2003.
[7] G. Heise, H. W. Schneider, and P. C. Clemens, "Optical Phased Array Filter Module With Passively Compensated Temperature Dependence, " in Proc. ECOC, pp. 319–320, 1998.
[8] N. Ooba, Y. Hibino, Y. Inoue, and A. Sugita, "A Thermal Silica-Based Arrayed-Waveguide Grating Multiplexer Using Bimetal Plate Temperature Compensator, " Electron. Lett., Vol. 36, pp. 1800–1801, 2000.
[9] W. Fleming, "Dispersion in GeO2-SiO2 Glasses, " Applied Optics, Vol. 23, No. 24, pp. 4486-4493, 1985.
[10] T. Ishigure, E. Nihei, and Y. Koike, "Optimum Refractive Index Profile of The Grade-Index Polymer Optical Fiber, Toward Gigabit Data Link, " Appl. Opt., Vol. 35, No. 12, pp. 2048-2053, 1996.
[11] D. H. Jundt, "Fabrication Techniques of Lithium Niobate Waveguides, " Optics Letters, Vol. 22, No. 9, pp. 1553, 1997.

## Appendix A

We can fit (dn/dT) as a function of three terms based on MATLAB curve-fitting program [9]:

$$\frac{dn}{dT} = d_0 + d_1\, l + d_2\, l^2 \qquad \text{(A1)}$$

The fitting based on no. of 17 points iteration at 300 K:

$$\frac{dn}{dT} = 0.66x10^{-4} - 0.67x10^{-4}\, l + 0.42x10^{-4}\, l^2 \qquad \text{(A2)}$$

The fitting based on no. of 17 points iteration at 305 K:

$$\frac{dn}{dT} = 0.59x10^{-4} - 0.59x10^{-4}\, l + 0.39x10^{-4}\, l^2 \qquad \text{(A3)}$$

The fitting based on no. of 17 points iteration at 310 K:

$$\frac{dn}{dT} = 0.58x10^{-4} - 0.59x10^{-4}\, l + 0.4x10^{-4}\, l^2 \qquad \text{(A4)}$$

The fitting based on no. of 17 points iteration at 315 K:

$$\frac{dn}{dT} = 0.58x10^{-4} - 0.58x10^{-4}\, l + 0.38x10^{-4}\, l^2 \qquad \text{(A5)}$$

The fitting based on no. of 17 points iteration at 320 K:

$$\frac{dn}{dT} = 0.57x10^{-4} - 0.57x10^{-4}\, l + 0.37x10^{-4}\, l^2 \qquad \text{(A6)}$$

The Root Mean Square (r. m. s) for fitting these equations is approximately (0.045 %).

The values of the coefficients with the operating temperature of Silica-doped as in **Table (1)**.

| T (K) | $d_0$ | $d_1$ | $d_2$ |
|---|---|---|---|
| 300 | 0.66x10$^{-4}$ | -0.67.x10$^{-4}$ | 0.42x10$^{-4}$ |
| 305 | 0.59x10$^{-4}$ | -0.59x10$^{-4}$ | 0.39x10$^{-4}$ |
| 310 | 0.58x10$^{-4}$ | -0.59x10$^{-4}$ | 0.4x10$^{-4}$ |
| 315 | 0.58x10$^{-4}$ | -0.58x10$^{-4}$ | 0.38x10$^{-4}$ |
| 320 | 0.57x10$^{-4}$ | -0.57x10$^{-4}$ | 0.37x10$^{-4}$ |

Table (1)

Then the fitting the values in the **Table (1)** to indicate the coefficients ( $d_0, d_1, d_2$ ) as a function of Temperature as follow:

$$d_0 = 0.72x10^{-2} - 0.46x10^{-4}T + 0.74x10^{-7}T^2 \qquad \text{(A7)}$$

$$d_1 = -0.7x10^{-2} - 0.45x10^{-4}T + 0.72x10^{-7}T^2 \qquad \text{(A8)}$$

$$d_2 = 0.1x10^{-2} - 0.63x10^{-5}T + 0.99x10^{-8}T^2 \qquad \text{(A9)}$$

## Appendix B

We can fit the relation between the variation of the refractive-index w. r. t the variation of Temperature (dn/dT) as a function of three terms based on MATLAB curve-fitting program [9]: $\frac{dn}{dT} = h_0 + h_1\, l + h_2\, l^2$ (B1)

The fitting based on no. of 17 points iteration at 300 K:

$$\frac{dn}{dT} = 0.42X10^{-2} - 0.78X10^{-3}\, l + 0.39x10^{-3}\, l^2 \qquad \text{(B2)}$$

The fitting based on no. of 17 points iteration at 305 K:

$$\frac{dn}{dT} = 0.41X10^{-2} - 0.77X10^{-3}\, l + 0.38x10^{-3}\, l^2 \qquad \text{(B3)}$$

The fitting based on no. of 17 points iteration at 310 K:

$$\frac{dn}{dT} = 0.4X10^{-2} - 0.75X10^{-3}\, l + 0.37x10^{-3}\, l^2 \qquad \text{(B4)}$$

The fitting based on no. of 17 points iteration at 315 K:

$$\frac{dn}{dT} = 0.39X10^{-2} - 0.74X10^{-3}\, l + 0.36x10^{-3}\, l^2 \qquad \text{(B5)}$$

The fitting based on no. of 17 points iteration at 320 K:

$$\frac{dn}{dT} = 0.38X10^{-2} - 0.72X10^{-3}\, l + 0.33x10^{-3}\, l^2 \qquad \text{(B6)}$$

The Root Mean Square (r. m. s) for fitting these equations is approximately (0.028 %).

The values of the coefficients with the operating Temperature of PMMA as in **Table (2)**.

| T (K) | $h_0$ | $h_1$ | $h_2$ |
|---|---|---|---|
| 300 | 0.42x10$^{-3}$ | -0.78x10$^{-3}$ | 0.39x10$^{-3}$ |
| 305 | 0.41x10$^{-3}$ | -0.77x10$^{-3}$ | 0.38x10$^{-3}$ |
| 310 | 0.4x10$^{-3}$ | -0.75x10$^{-3}$ | 0.37x10$^{-3}$ |
| 315 | 0.39x10$^{-3}$ | -0.74x10$^{-3}$ | 0.36x10$^{-3}$ |

| | | | |
|---|---|---|---|
| 320 | $0.38x10^{-3}$ | $-0.72x10^{-3}$ | $0.33x10^{-3}$ |

Table (2)

Then the fitting the values in the **Table (2)** to indicate the coefficients ( $h_0, h_1, h_2$ ) as a function of Temperature as follow:

$$h_0 = 0.13x10^{-2} - -0.42x10^{-5}T + 0.41x10^{-8}T^2 \quad \text{(B7)}$$

$$h_1 = -0.3x10^{-2} + 0.12x10^{-4}T - 0.13x10^{-7}T^2 \quad \text{(B8)}$$

$$h_2 = 0.16x10^{-2} - 0.65x10^{-5}T + 0.82x10^{-8}T^2 \quad \text{(B9)}$$

## Appendix C

We can fit the variation of the refractive-index w. r. t the variation of the temperature (dn/dT) as a function of three terms based on curve-fitting program [9]:

$$\frac{dn}{dT} = y_0 + y_1 l + y_2 l^2 \quad \text{(C1)}$$

The fitting based on no. of 17 points iteration at 300 K:

$$\frac{dn}{dT} = 0.95X10^{-4} - 0.9X10^{-4} l + 0.34x10^{-4} l^2 \quad \text{(C2)}$$

The fitting based on no. of 17 points iteration at 305 K:

$$\frac{dn}{dT} = 0.99X10^{-4} - 0.959X10^{-4} l + 0.37x10^{-4} l^2 \quad \text{(C3)}$$

The fitting based on no. of 17 points iteration at 310 K:

$$\frac{dn}{dT} = 0.997X10^{-4} - 0.956X10^{-4} l + 0.372x10^{-4} l^2 \quad \text{(C4)}$$

The fitting based on no. of 17 points iteration at 315 K:

$$\frac{dn}{dT} = 0.1X10^{-3} - 0.96X10^{-4} l + 0.373x10^{-4} l^2 \quad \text{(C5)}$$

The fitting based on no. of 17 points iteration at 320 K:

$$\frac{dn}{dT} = 0.103X10^{-3} - 0.98X10^{-4} l + 0.38x10^{-4} l^2 \quad \text{(C6)}$$

The Root Mean Square (r. m. s) for fitting these equations is approximately (0.055 %).

The values of the coefficients with the operating Temperature of $LiNbO_3$ as in **Table (3)**.

| T (K) | $y_0$ | $y_1$ | $y_2$ |
|---|---|---|---|
| 300 | $0.95x10^{-3}$ | $-0.9x10^{-3}$ | $0.34x10^{-3}$ |
| 305 | $0.99x10^{-3}$ | $-0.95x10^{-3}$ | $0.37x10^{-3}$ |
| 310 | $0.997x10^{-3}$ | $-0.959x10^{-3}$ | $0.372x10^{-3}$ |
| 315 | $0.1x10^{-3}$ | $-0.96x10^{-3}$ | $0.373x10^{-3}$ |
| 320 | $0.103x10^{-3}$ | $-0.98x10^{-3}$ | $0.38x10^{-3}$ |

Table (3)

Then the fitting the values in the **Table (3)** to indicate the coefficients ( $y_0, y_1, y_2$ ) as a function of Temperature as follow:

$$y_0 = -0.12x10^{-2} - 0.77x10^{-5}T - 0.12x10^{-7}T^2 \quad \text{(C7)}$$

$$y_1 = 0.31x10^{-2} - 0.2x10^{4}T + 0.32x10^{-7}T^2 \quad \text{(C8)}$$

$$y_2 = -0.15x10^{-2} + 0.1x10^{-4}T - 0.16x10^{-7}T^2 \quad \text{(C9)}$$

**Abd-Elnaser A. Mohammed** Received Ph.D degree from the faculty of Electronic Engineering, Menoufia University in 1994. Now, his job career is Assoc. Prof. Dr. in Electronics and Electrical CommunicationEngineering department. Currently, his field and research interest in the passive optical communication Networks, digital communication systems, and advanced optical communication networks.

**Ahmed Nabih Zaki Rashed** was born in Menouf, Menoufia State, Egypt, in 1976. Received the B.Sc. and M.Sc. scientific degrees in the Electronics and Electrical Communication Engineering Department from Faculty of Electronic Engineering, Menoufia University in 1999 and 2005, respectively. Currently, his field interest and working toward the Ph.D degree in Active and Passive Optical Networks (PONs). His research mainly focuses on the transmission data rate of optical networks.